ELSEVIER

Journal of Structural Geology 30 (2008) 354–365

JOURNAL OF STRUCTURAL GEOLOGY

www.elsevier.com/locate/jsg

Geometrical analysis of the Punta del Pedrón shear zone (Asturias, Spain): Implications related to exploration of Salave Gold-type mineralization ☆

Pablo Gumiel [a,b,*], Agustín Martín-Izard [c], Mónica Arias [b], Luis Rodríguez-Terente [c]

[a] *Dir. Recursos Min. IGME, Ríos Rosas 23, 28003 Madrid, Spain*
[b] *Department of Geology, Facultad de Ciencias, (A-2, km 33,600), 28871 Alcalá de Henares, Madrid, Spain*
[c] *Department of Geology, University of Oviedo, C/Arias de Velasco s/n, 33005 Asturias, Spain*

Received 27 March 2007; received in revised form 14 November 2007; accepted 23 November 2007

Abstract

The Salave Gold deposit is located at the northern end of the Oscos Gold Belt which forms part of the Asturian-Leonese Zone of the Variscan Massif. The Gold Belt and the Salave deposit are genetically related to the emplacement of post-kinematic granitoids which were largely controlled by Variscan fracture systems. A geometrical analysis following the McCoss [McCoss, A.M., 1986. Simple construction for deformation in transpression/transtension zones. Journal of Structural Geology 8(6), 715–718] method has been utilized to discriminate the transpressional, transtensional, and simple shear components, and the displacement vectors (S-vectors) of the Punta del Pedrón shear zone. A contour map of the S-vector orientations is consistent with the contour map of the calculated extension of the whole area, and shows those shear zones where extensional and contractional components have been determined. Extension is higher ($E = 15\%$) towards the east where transtension is predominant near the Salave gold deposit. This deposit is located at the intersection of the extensional sinistral shear zones striking between 130° and 140°, which promoted dilation and the emplacement of the Salave granodiorite, with the dextral shear zones striking between 070° and 080°. Extension was transferred to the dextral shear zones, and associated 030° pinnate veins, in a transtensional stage which promoted connected vein systems and localized fluid-flow. This gave rise to the alteration patterns of the deposit and ore deposition in an area previously affected by the Mondoñedo thrust system. The use of this geometrical method, with limitations and several assumptions discussed in the text, and the analysis of the scaling properties of the vein sets in traverses can be utilized in the field to aid in mineral exploration.

Keywords: Shear; Geometry; Fractal; Salave; Veins; Compression; Extension

1. Introduction

The Romans recognized 2000 years ago that the northwest of the Iberian Peninsula was an important gold province. During the 19th and 20th centuries, all activity was centred on gold-bearing quartz-arsenopyrite vein systems. With an estimated historical production in excess of 3 million ounces of gold and an existing global resource of 4.2 million ounces (Spiering et al., 2000), the region has rewarded the persistent explorer since the dawn of recorded history. The most recent exploration started in the sixties, culminating in the discovery by Río Narcea Gold Mines of the El Valle and Carlés deposits, and also the Salave deposit which was being prepared for exploitation. However, to date, authorization has not been given by the regional government (Fig. 1A,B).

The gold deposits identified in western Asturias and Galicia were formed by multiple gold mineralizing events representing several styles of mineralization in a structurally complex, but

☆ Based on this paper, an oral communication was presented at the 12th Quadrennial IAGOD symposium 2006: Understanding the genesis of ore deposits to meet the demands of the 21st Century, Moscow 2006.

* Corresponding author. Department of Geology, Facultad de Ciencias, (A-2, km 33,600), University of Alcalá, 28871 Alcalá de Henares, Madrid, Spain. Tel.: +34 918854997; fax: +34 918855090.
E-mail address: pablo.gumiel@uah.es (P. Gumiel).

0191-8141/$ - see front matter © 2007 Elsevier Ltd. All rights reserved.
doi:10.1016/j.jsg.2007.11.009

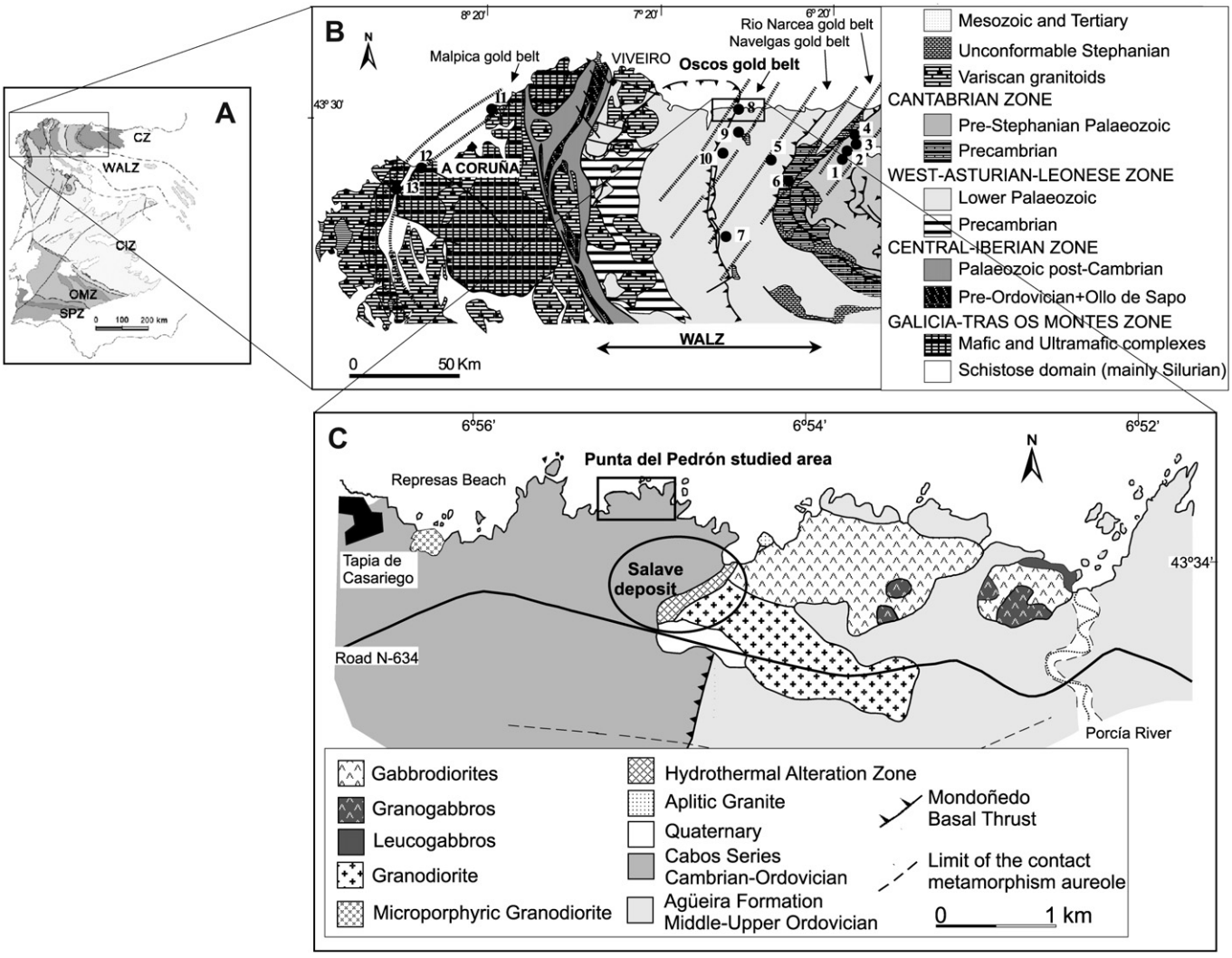

Fig. 1. (A) The Iberian Massif. CZ: Cantabrian Zone, WALZ: West-Asturian Leonese Zone, CIZ: Central Iberian Zone, OMZ: Ossa Morena Zone, SPZ: South Portuguese Zone. (B) Regional geology of the NW Iberian Peninsula with the situation of the main gold deposits: (1) El Valle-Boinás, (2) Mari Luz y La Brueba, (3) Carlés, (4) Ortosa y Godán, (5) La Freita, (6) Linares, (7) Ibias, (8) Salave, (9) Ouria, (10) Pena Porto, (11) Chousa, (12) Covas, (13) Corcuesto. (C) Geological sketch of the Salave gold area within the Oscos Gold Belt.

favorable terrain of Paleozoic carbonate and clastic host rocks. Numerous previous works have been published about other deposits in the Asturias region (e.g. Spiering et al., 2000; Cepedal et al., 2000; Fuertes-Fuente et al., 2000; Martin-Izard et al., 2000a,b), but to date no detailed articles have been published on the Salave gold deposit. Only descriptive models of Salave have been published (Harris, 1979, 1980a,b; Fernández-Catuxo, 1998; Rodríguez-Terente et al., 1998) and little is known about the structural characteristics of this intrusion-related gold system (Lang and Baker, 2001).

The Salave deposit is located close (500 m) to the Cantabrian coast where outcropping host-rocks permit a detailed study of several types of shear structures. For a better understanding of the Salave deposit, where (Au-Mo) vein geometry, and emplacement is largely conditioned by regional fractures and shears, an analysis of the Punta del Pedrón shear zones has been undertaken using the McCoss (1986) method. This author in his original work specified that the analysis assumes that in triaxial strain volume is conserved. He also stipulated that lateral extrusion or intrusion of material from or into the shear zone is not allowed, and the material is permitted to thicken and thin vertically. We assumed in our work, that in transtensional arrays net volume may increase if vein material is introduced into the shear zones, and conversely, net volume may decrease in transpressional zones if material is removed (e.g. Peacock and Sanderson, 1995).

The use of the McCoss's method in this contribution, with the assumptions mentioned above, has revealed the existence of contractional and extensional areas. The latter areas are more likely to explain the occurrence of the (Au-Mo) mineralization. Discrimination of extensional deformation is consistent with fracture connectivity using the scaling properties of the vein arrays in the available exposures.

2. Regional geology

The Iberian Massif (Fig. 1A) presents the westernmost exposures of the European Variscan Belt in the south-western limb of the arc of this chain in Western Europe, and it provides the most complete section from the external to the internal parts of the orogen. It is a collisional belt that has been divided into five zones (Julivert et al., 1972) which represent the footwall of the suture. The Salave gold deposit is located in the West Asturian-Leonese Zone, within what is locally known as the Oscos Gold Belt.

The West Asturian-Leonese Zone (WALZ – Fig. 1B) represents a transition between the foreland areas to the east (Cantabrian Zone) and the internal zones to the west (Central Iberian Zone). Its sedimentary rocks consist of a thick pre-orogenic sequence comprising the whole of the Cambrian, Ordovician and Silurian. This sequence lies unconformably upon Upper Proterozoic turbiditic terrigenous sediments.

The WALZ was affected by three coaxial deformation phases related to a roughly E-W trending shortening (Martínez-Catalán et al., 1990). The first (D_1) produced large recumbent and overturned folds, and a generalized slaty cleavage (S_1). The second (D_2) was responsible for thrust-type structures and associated shear zones. The third (D_3) gave rise to large open folds, approximately homoaxial with the D_1 folds, and also crenulation cleavage (S_3), intense fracturing and shear zones. Regional metamorphism increases towards the west from greenschist to amphibolite facies. Variscan granitoids are abundant in the western part and can be divided into two main groups: syntectonic and post-tectonic (Corretgé and Suárez, 1990). The Salave deposit is related to the post-tectonic association.

Fractures controlled the orientation of the gold deposits, which form NE-SW trending belts (Spiering et al., 2000) that created weakness zones for gold concentration. In each gold belt the style of mineralization is different, and from an economic point of view the most important are the Río Narcea and Oscos gold belts (Fig. 1B). Within each belt several east-west, northwest, and northeast fault systems exhibit a long history of movement (reactivations) in the region, with traces affecting numerous stratigraphic units. These structures show both local and regional control on the site of gold deposition, and control the emplacement of several small post-orogenic calc-alkaline igneous intrusions (Corretgé and Suárez, 1990) ranging in composition from gabbro to granite. The Oscos Gold Belt forms a 20 km wide belt of gold occurrences with several Roman workings. At the northern end of the belt, gold mineralization has been identified as intrusive-hosted ore at Salave (Fig. 1B,C).

3. The Salave Gold deposit

Geological exploration and drilling in the Oscos Belt have been concentrated in the Salave gold deposit (approximately 30,000 meters of drilling in 170 holes define an estimated resource of 1.9 million ounces of gold in 20.5 million tonnes of material averaging 2.9 g/t Au), representing one of the largest unexploited gold deposits in western Europe. The old workings are calculated to have removed roughly 4–5 million tons of ore. Salave was also exploited for molybdenum during the Second World War. Although Salave is well known from an economic point of view, only a general descriptive model has been published (Harris, 1979, 1980a,b; Fernández-Catuxo, 1998; Rodríguez-Terente et al., 1998) and little is known about the structural characteristics of mineralization. The gold mineralization is localized in the roof of a small post-tectonic I-type plutonic complex just where the Mondoñedo thrust reaches the Cantabrian Sea (Fig. 1C). This complex consists of a granodiorite to quartz-diorite and tonalite that intrudes a gabbroic body. Both granites and gabbros are hosted by strongly fractured Cambrian-Ordovician siliciclastic metasediments of the Los Cabos series and the Agüeira Formation, which in the area are separated by the Mondoñedo thrust.

The granodiorite is volumetrically the main host-rock of the ore deposit and belongs to the post-tectonic granodiorite-monzogranite stocks (Fernández-Suárez, 1998). The Salave granitoid shows a WNW-ESE elongated geometry normal to the Variscan structures in the area, and this geometry is probably conditioned by the 130°–140° trending fractures and shear zones. The granodiorite is intensely altered at its western end (Fig. 1C), where the Romans exploited the gold, and their open-cast mine follows roughly a NE-SW trending geometry parallel to the Variscan structures, including the Mondoñedo thrust.

As defined by Fernández-Catuxo (1998) and Rodríguez-Terente et al. (1998) and based on the results of drill cores, the geometry of the mineralized body is approximately tabular (a network of fractures controlling the mineralized levels dipping to the W – Fig. 2), roughly parallel to the Mondoñedo thrust.

Intrusions and host-rocks were affected by later faulting and fracturing, and several of these fractures controlled the Salave mineralization. The hydrothermal phenomenon related to the intrusion is mainly located to the western end, and is focused along the fracture system probably related to the reactivation of the Mondoñedo thrust (Fig. 3A). The Salave granodiorite was affected by intense hydrothermal alteration, albitization and strong sericitization around fractures, and chloritic-propylitic alteration within the granodiorite (Fig. 2) which resulted in textural, mineralogical and chemical transformations, and is associated with the introduction of metals of economic interest (Mo, Au – Fig. 3B).

4. Geometrical analysis of the Punta del Pedrón shear zone

The Salave deposit is covered by the abundant quaternary sediments of the area, the old Roman and recent mining slags and tailings, trees around the open cast mine and water inside it and has only scarce rock outcrops. By contrast, the cliffs at the nearby coast (less than 500 m away) allow a clear view of the rocks and of the structures affecting them. In particular, the Punta del Pedrón area is probably the best place close by (within 1 km) affected by the regional Variscan fracturing for us to perform a geometrical study of their

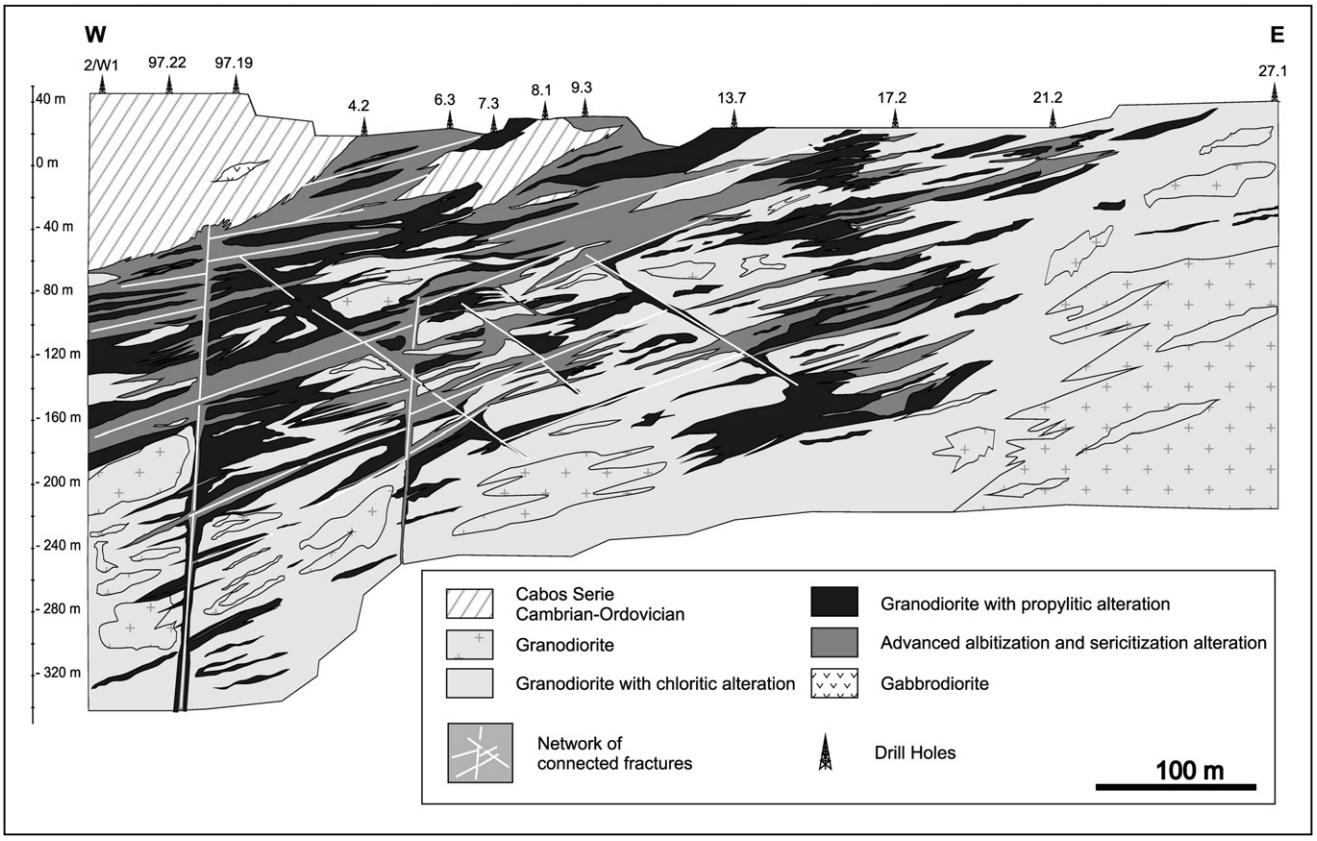

Fig. 2. Idealized geometry of the Salave ore deposit. Network of connected fractures and faults controlled hydrothermal alteration and vein systems preferently at the contact with the metasediments. The geometrical model has been obtained from borehole data.

characteristics and infer possible relationships with the mineralized area.

A geometrical analysis following the McCoss (1986) method has been utilized to determine the transpressional, transtensional, and simple shear components, and the displacement vectors (S-vectors) of the Punta del Pedrón shear zone. Detailed structural mapping of the different shear zones has involved georeferencing in a coordinate grid obtained by GPS and a synthesis of the information using GIS. The geometrical analysis was undertaken in an area covering 230 m × 70 m (Fig. 4A), and detailed structural mapping of the vertical shear zones has been carried out on an outcrop to the west 45 m × 15 m in size, in the available exposures and cliff conditions, in the Cambrian-Ordovician siliciclastic metasediments of the Los Cabos Fm (Fig. 3C). The S vectors have been obtained from the McCoss (1986) method using the tips of the sigmoidal semi-brittle to ductile en-échelon tension gash veins (Fig. 3D,E). By assuming that the relatively undilated and unrotated ends of fractures are parallel to the orientation of the minimum principal axis of the infinitesimal sectional strain ellipse, this method can be used to find the zone boundary displacement vector.

In this two-dimensional analysis of sigmoidal vein arrays, we are describing oblique convergence or oblique divergence in the shear zones, and the McCoss (1986) method relates principal incremental strain to wall rock displacement. When the zone is extensional or slightly transtensional (Fig. 3E), originally en-échelon veins link by extension fractures breaking across bridges, without shear or pressure solutions. As shear increases, the bridges can break by shear fracturing with some pressure solutions occurring at $\hat{A}$ angles as low as 142° (Fig. 3E). Because simple shear involves no volume change, it is probable that volume loss caused by pressure solution approximately equals volume increase by veining.

The McCoss's method is illustrated in Fig. 3E, assuming that the vein tips represent Mode I cracks (which propagate perpendicular to the minimum principal stress, σ_3). The procedure is as follows: 1) Draw the boundaries to the zone. 2) From the tip of the sigmoides, draw a line parallel to the vein long axis. The angle between this line and the zone boundary is ω. 3) Draw a circle outside the zone, with the diameter perpendicular to the zone boundary at the intersecting point of the zone and the line parallel to the vein. 4) Draw a line from the intersecting point of the prolongation of the vein through the center of the circle to the other side of the circle. This line gives the infinitesimal displacement vector (S-vector).

The following relationship exists: $\hat{A} = 180° - 2\omega$, where $\hat{A}$ is the infinitesimal displacement direction and ω is the angle between the vein segments and the zone boundary. $\hat{A}$ varies from 180° for plane extension to 0° for plane contraction. $\hat{A}$ between 0° and 90° is transpression, $\hat{A} = 90°$ is simple shear,

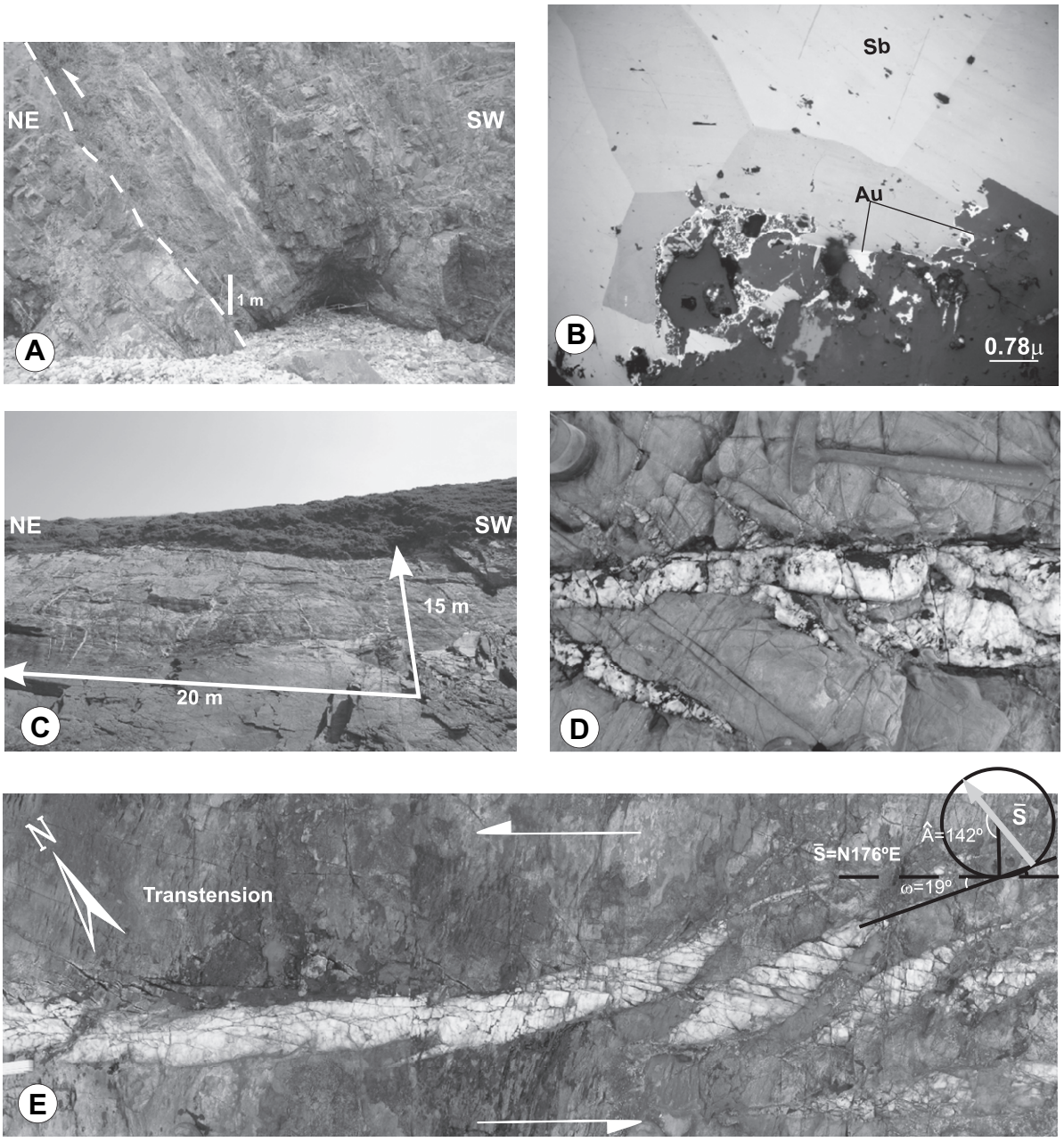

Fig. 3. (A) A reverse fault probably related to the Mondoñedo thrust system. (B) Photomicrograph of a polished section of Stibnite (Sb) and gold (Au). (Reflected light). (C) A partial view of the shear zones of the Punta del Pedrón outcrop, western part of the studied area. (D) Different generation of en-échelon veins. Extensional veins are nucleated and developed over contractional vein arrays. E). Application of the geometrical McCoss (1986) method to obtain the displacement (S vector) using the tips of the sigmoidal semi-brittle to semiductile en-échelon extensional veins (for explanation see text). Notice the bridge-bending process promoted by Nicholson and Pollard (1985) to accommodate crack dilation in those shears where extension is predominant.

and $\hat{A}$ between 90° and 180° is transtension (Peacock and Sanderson, 1995).

In the studied area, 34 displacement vectors (S-vectors, Fig. 4B) and the direction of the infinitesimal displacement ($\hat{A}$) were obtained (Table 1).

An idealized kinematic model with the location of the maximum shortening direction $\sigma_1 = 105°$ and maximum extension direction ($\sigma_3 = 015°$) has been postulated which agrees with the orientation and distribution of late-variscan shear zones in the area (Fig. 4C).

Fig. 4. (A) Topographic contours (0, 10, 20 m above sea level) of the whole area showing the location of the studied zones (black and white dots are respectively contractional and extensional components). (B) Detailed structural mapping of the different shear zones georeferenced in a coordinate grid obtained by GPS in the Punta del Pedrón outcrop of 45 m × 15 m in the Cambrian-Ordovician siliciclastic metasediments of the Los Cabos Fm (black and grey vectors are contractional and extensional vectors respectively). (C) Idealized kinematic model with the location of the maximum shortening direction $\sigma_1 = 105°$ and maximum extension direction $\sigma_3 = 015°$ of the Punta del Pedrón shear zone (C scale is different of B).

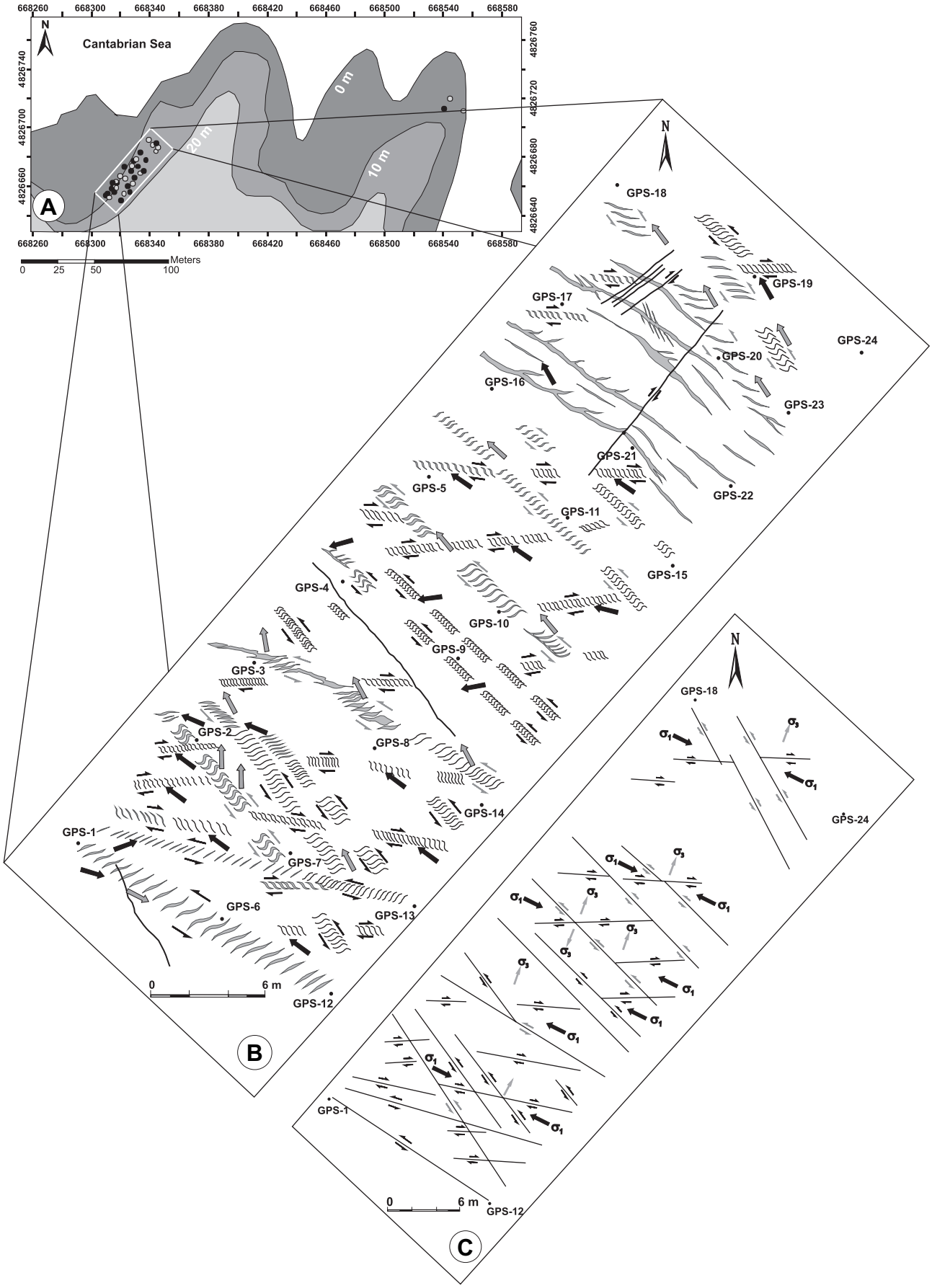
668260
668300
668340
668380
668420
668460
668500
668540
668580
4826760
4826740
4826720
4826700
4826680
4826660
4826640
N
Cantabrian Sea
0 m
20 m
10 m
A
Meters
0
25
50
100
GPS-18
GPS-19
GPS-17
GPS-24
GPS-20
GPS-16
GPS-23
GPS-21
GPS-5
GPS-22
GPS-11
GPS-15
GPS-4
GPS-10
GPS-9
GPS-3
GPS-2
GPS-8
GPS-14
GPS-1
GPS-7
GPS-6
GPS-13
GPS-12
0
6 m
B
C
σ1
σ3

Table 1
Displacement vectors measured in the studied area

Component of the shear zones	S-vector orientation	$\hat{A}$ (infinitesimal displacement orientation)	Extension (E%)
OC	N 104° E	27°	5
OD	N 120° E	106°	15
OC	N 140° E	29°	5
OC	N 70° E	83°	5
OD	N 158° E	171°	15
OC	N 140° E	16°	5
OC	N 138° E	66°	5
OC	N 138° E	68°	5
OD	N 178° E	119°	15
OD	N 180° E	140°	15
OC	N 140° E	29°	5
OC	N 140° E	37°	5
OD	N 160° E	165°	15
OD	N 158° E	157°	15
OC	N 134° E	48°	5
OD	N 176° E	99°	15
OD	N 160° E	151°	15
OC	N 80° E	32°	5
OD	N 148° E	117°	15
OC	N 100° E	40°	5
OC	N 75° E	17°	5
OC	N 70° E	27°	5
OD	N 148° E	96°	15
OC	N 130° E	72°	5
OC	N 130° E	85°	5
OD	N 145° E	149°	15
OC	N 130° E	36°	5
OC	N 150° E	13°	5
OD	N 154° E	140°	15
OD	N 154° E	138°	15
OD	N 150° E	97°	15
OD	N 154° E	120°	15
OD	N 157° E	18°	5
OD	N 70° E	136°	15

Component of the shear zones, S-vector orientation, $\hat{A}$ (infinitesimal displacement orientation) and extension (E%) by traverses. OC = oblique convergence, OD = oblique divergence.

A contour map with the orientation of S-vectors has been generated for the western outcrop (Fig. 5A,B), and shows the contractional (dark grey colours) and extensional (light grey colours) components of the shear zones. The contractional (transpressional) are arranged as roughly linear features. However, the extensional (transtensional) segments are distributed as circular features, and are predominant towards the east where the Salave gold mine is located. This area can be interpreted as favourable for the emplacement of the Salave type of granitoids, and probably localized high flow in dilation zones promoting fluid-flow and ore deposition.

Extension (E) has been calculated from veins in those traverses where S-vectors were obtained (Table 1), following the equation:

$$E = \left(\frac{\sum \mathrm{vth}}{(\mathrm{lTr} * 1000) - \sum \mathrm{vth}} \right) \times 100 \qquad (1)$$

where vth = vein thickness (mm), and lTr = length of the traverses (m).

Extension is higher ($E = 15\%$) in those shear zones where transtension is predominant, and is lower ($E < 5\%$) in those where transpression is the principal component. A contour map of E has been obtained and shows that extension increases towards the east (Fig. 5C) near the Salave gold deposit. The detailed contour map of the S-vector orientations (Fig. 5B) is consistent with the general contour map of the quantified extension E (Fig. 5C), and with the contour map of the infinitesimal displacement orientation $\hat{A}$ (Fig. 5D) over the whole area.

4.1. Scaling of Punta del Pedrón shear zone

Vein thickness distributions have been widely studied during the past few years (e.g. Sanderson et al., 1994; Gumiel et al., 1995; Johnston and McCaffrey, 1996; McCaffrey and Johnston, 1996; Roberts et al., 1998, 1999), and have generally been found to conform to power-law distributions. Sigmoidal tension gash data were collected along ten traverses across exposures of shear zones, usually approximately normal to the vein set. The position of the intersection of the veins along the traverse was recorded, together with its thickness (in the central part of the tension gashes), orientation and length. Thus tension gash arrays have been analyzed in terms of their scaling properties considering size distributions (length, thickness) and measurement of spacing distribution.

Cumulative frequency plots of vein thickness have been compared with various distribution models (normal, log-normal, negative-exponential and power-law). Many vein systems conform to power-law distributions (e.g. Sanderson et al., 1994; Clark et al., 1995; Gillespie et al., 1999; Roberts et al., 1999) where the number of veins per metre (N_t) of thickness $\geq t$ is of the form:

$$N_i \approx C t^{-D_t} \qquad (2)$$

where C represents the density of veins with ≥ 1 mm thickness and D_t is a scaling exponent often referred to as the fractal dimension of the distribution. Thus a plot of $\log(N_t)$ against $\log(t)$ is a straight line of slope $-D_t$ for a power-law distribution.

Data for vein thickness of the tension gashes from the study area are shown in Fig. 6A,B. Locally, for individual shears, the thickness distribution conforms to negative-exponential distributions that can be interpreted, as the tension gashes initiate randomly in a shear, and also may show characteristic length scales, usually with log-normal distributions, but generally, these plots show power-law distributions with various departures from an ideal power-law, attributable to truncation (non-sampling) of small thicknesses and to the finite range of thickness over which veins are developed (Pickering et al., 1996).

Vein thickness in the study area is in the range 1–430 mm, and the values of the thickness distribution fractal dimension D_t estimated for the two outcrops are different. $D_t = 0.86$ (Fig. 6A) from the tension gash arrays in the western outcrop

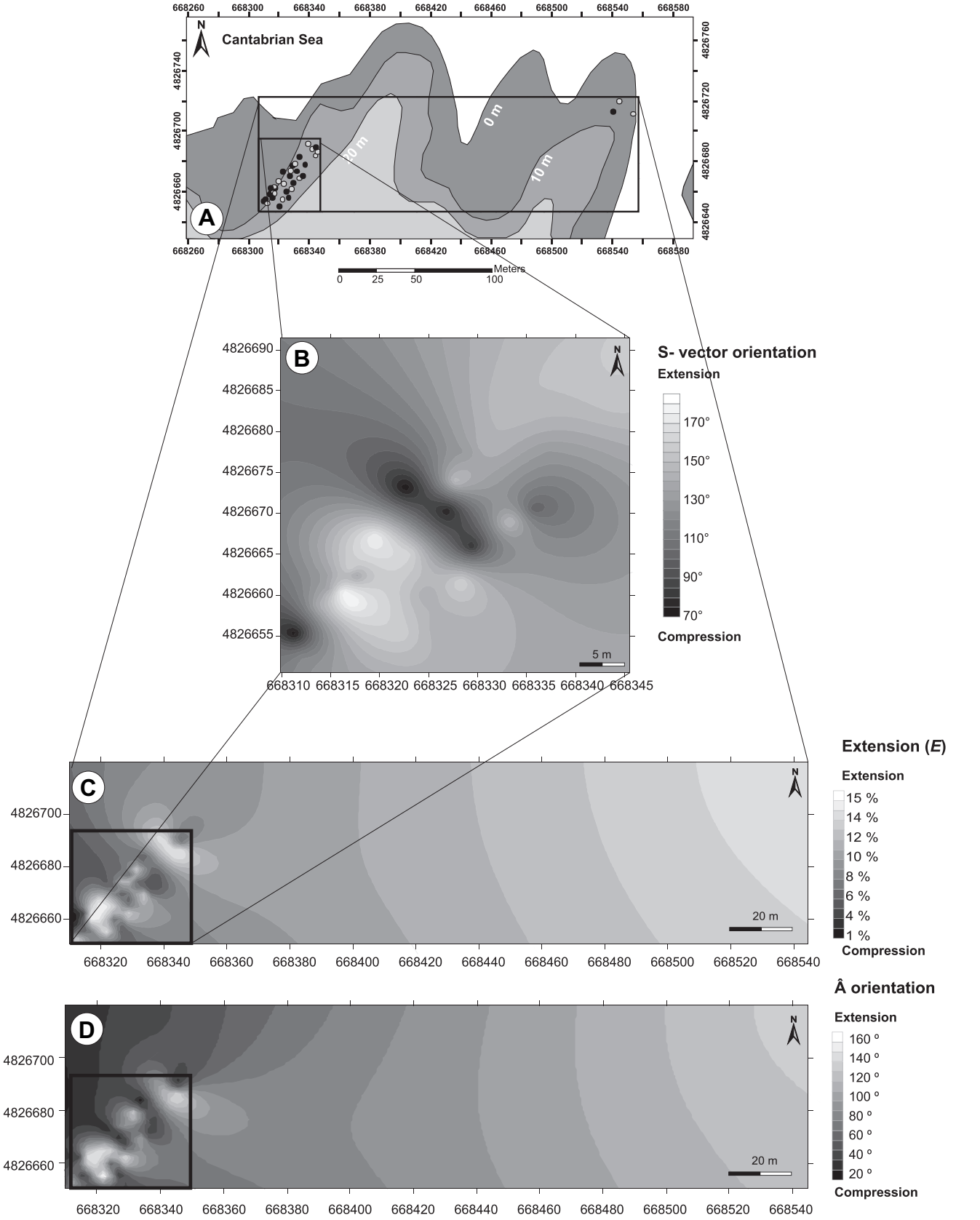

Fig. 5. (A) Topographic contours (0, 10, 20 m above sea level) over the whole area showing the location of the studied zones. The big rectangle corresponds to parts C and D, and the small is part B. (B) Contour map showing the orientation of contractional (dark grey colours) and extensional (light grey colours) components (S-vectors) of the Punta del Pedrón shear zone, western part of the studied area. (C) Contour map of the calculated extension (E) from veins in traverses over the whole area. (D) Contour map of the infinitesimal displacement orientation ($\hat{A}$) over the whole area. Dark grey colours are contractional components and light grey colours are extensional components.

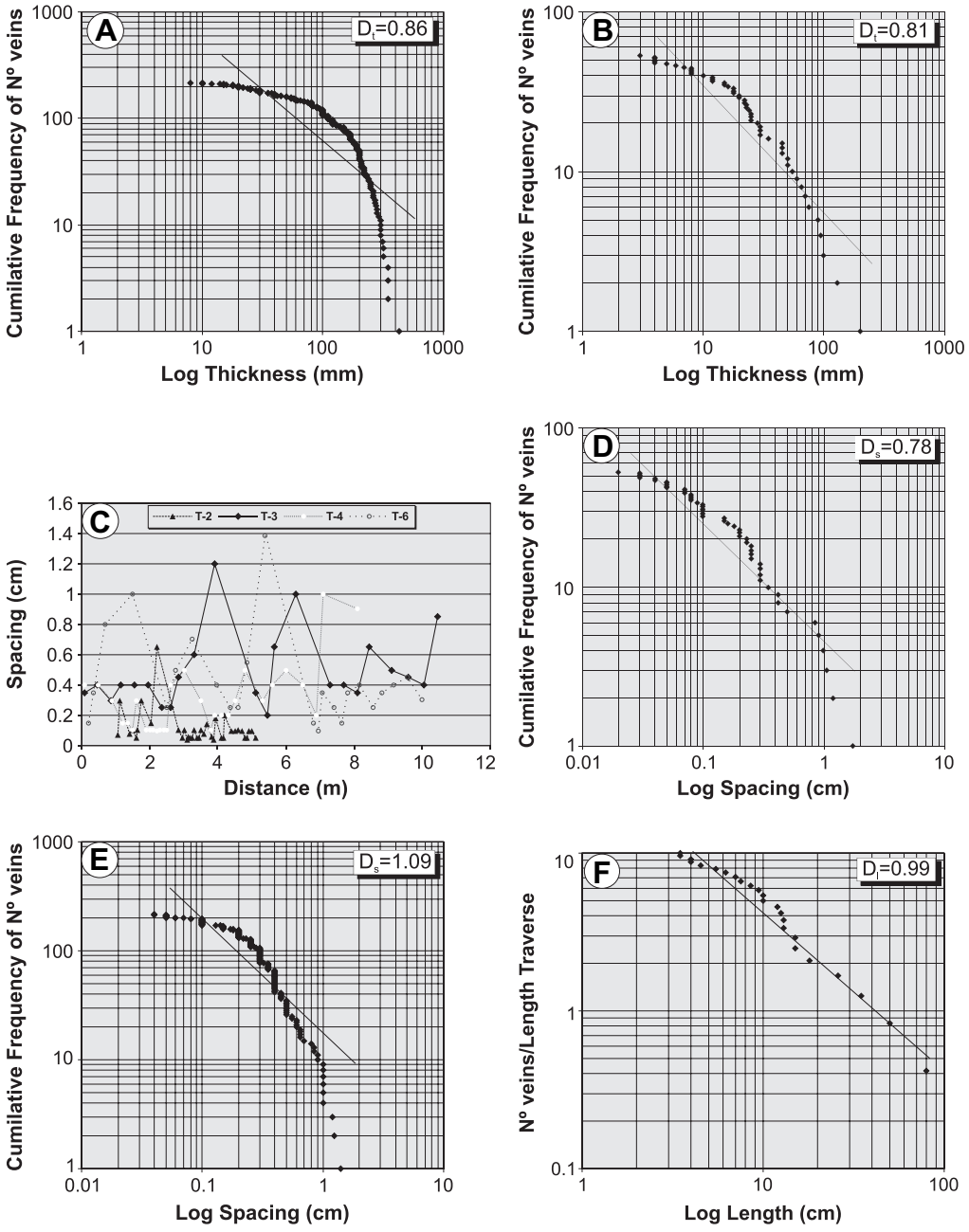

Fig. 6. (A) Vein thickness distribution from tension gash arrays in the western outcrop (Punta del Pedrón shears). (B) Vein thickness distribution from tension gash arrays in the eastern area. (C) Spacing of the tension gashes in several traverses from the study area suggests moderate amounts of clustering. (D) Spacing distribution in those systems where extension is predominant. (E) Spacing distribution in those systems where contraction is predominant. (F) Length distribution of tension gashes conform to power-law distributions (for explanation see text).

(Punta del Pedrón shears), and a lower value, $D_t = 0.81$ (Fig. 6B) has been obtained from sigmoidal tension gash arrays located in the eastern area. This can be expected, as the eastern sector shows well connected vein system near to the Salave deposit. These differences in thickness distribution are similar to those reported from other mineralized vein systems in Spain (Gumiel et al., 1995; Roberts et al., 1998, 1999).

Spacing distribution also conforms to power-law distribution of the form:

$$N_s \approx C s^{-D_s}, \tag{3}$$

where N_s is the number of tension gashes with a spacing $\geq s$, C represents the density of veins, and D_s is a scaling exponent often referred to as the fractal dimension of the distribution. Thus a plot of $\log(N_s)$ against $\log(s)$ is a straight line of slope $-D_s$ for a power-law distribution. Cumulative frequency plots of vein spacing (orthogonal distance between adjacent veins)

have also been compared with various distribution models (normal, log-normal, negative-exponential and power-law).

Data for spacing of the tension gashes from the study area suggests moderate amounts of clustering (Fig. 6C). This may be interpreted in terms of self-affine fractal scaling of tension gash geometry which has been verified at a variety of scales. D_s values, in the ranges of 0.02–1.5 cm, are lower ($D_s = 0.78$, Fig. 6D) in those systems where extension is predominant, and promotes the development of connected vein arrays capable of supporting high fluid-flow. However, higher D_s values ($D_s = 1.09$, Fig. 6E) correspond to less connected tension gash arrays in those shears where compression is predominant.

Tension gash length distribution sporadically conform to power-law distributions (fractal) with $D_l = 0.99$ in the range between 3 cm and 80 cm (Fig. 6F) in those shear zones where compression is predominant.

5. Evolution of the Punta del Pedrón shear zone

When an extension fissure system is developed during the initial shear displacement in simple shear, then the tension gashes are orientated orthogonal to the first maximum incremental extension, that is at 135° to the shear zone boundary, and form parallel en-echelon arrays (Ramsay and Huber, 1983, pp. 23–24). In the study area there are two main conjugate shear zones; dextral shear zones striking from 070° to 080°, and sinistral shear zones striking between 130° and 140° (Figs. 4B and 7A) developed at 30° to σ_1 orientated at 105° (Fig. 4C). Once formed, the fissures become carried along by subsequent displacements taking place in the shear zone, and their initial formation angle of 135° becomes reduced depending of the shear strain. Therefore the first fissures rotate, and as they are rotating become opened and filled with crystalline material deposited from pore fluids (quartz in this case).

As the shear zone widens and the deformation moves outwards, the fissure tips will propagate near the shear zone boundaries. The propagation direction will be controlled by the incremental strains and oriented at 135° to the shear zone. The total fissure geometry links the rotated central part of the vein with a 135° oriented tip and exhibits a sigmoidal shape (Fig. 7B). As the shear displacement at the zone centre becomes very large, it is possible that the central part of sigmoidal veins is badly oriented to allow stretching necessary along the direction of maximum incremental extension to accommodate deformation. At this stage a new cross-cutting vein set initiates at 135° to the shear zone boundaries, and the first vein system becoming inactive as the new extension system develops (Figs. 3D and 7C). The new cross-cutting vein set evolves in the same way as previous set developing a sigmoidal shape, as shear displacement at the zone centre becomes very large. Pressure solutions seams appear in those shear zones where contractional component is predominant.

The sinistral shear zones become more active, and their extensional component is predominant promoting dilation. This scenario is favourable for the emplacement of the Salave intrusive body with its elongated WNW-ESE trending geometry (Figs. 1C and 7D). The granodiorite sealed these shears, and extension was transferred mainly to the dextral shear zones, which became more active at this stage, hosting most of the Mo-mineralized veins. Their extensional components are predominant, and are nucleated and developed over contractional sigmoidal veins favouring dilation of extensional fractures (Figs. 3D and 7D). 030° pinnate veins are associated with the dextral shear zones and are coincident with the direction of the Mondoñedo thrust and the gold bearing system.

The scaling properties of the sigmoidal tension gashes at Punta del Pedrón are affected by the superimposition of oblique divergence over oblique convergence (Fig. 3D) which is critical for the emplacement of the Salave-type granitoids, and to localize fluid-flow and ore concentration.

6. Conclusions

The McCoss (1986) geometrical model has been demonstrated in the field to determine transpressional, transtensional, shear components and displacement vectors in semi-brittle to ductile sigmoidal en-échelon tension gash arrays. We have applied this method with caution to determine the orientation of the principal axes of the infinitesimal sectional strain ellipses in several transverses, and to discriminate extensional and contractional areas in the shear zones. A kinematic model with the location of the maximum shortening direction ($\sigma_1 = 105°$) and maximum extension direction ($\sigma_3 = 015°$) has been generated which agrees with the orientation and distribution of late-variscan shear zones in this part of the WALZ.

The calculated extension of the vein sets is higher ($E = 15\%$) in those shear zones where oblique divergence is predominant, and is lower ($E < 5\%$) in those where oblique convergence is the principal process. A contour map of the quantified extension (E) shows an increase of extension towards the east near the Salave gold deposit (Fig. 5C).

The detailed contour map of the S-vector orientations is consistent with the general contour map of the calculated extension (E) over the whole area. The transpressional zones are arranged as roughly linear features, and the transtensional areas are distributed as circular features, mainly located towards the east near the Salave gold deposit. This is to be expected, as extensional segments are favorable areas for the emplacement of the Salave-type of granitoids and also to localize fluid-flow in these dilation zones.

On a regional scale, the Salave gold deposit is located at the intersection of the extensional sinistral shear zones which promoted dilation and the emplacement of the Salave granodiorite (Fig. 7E) with the dextral shears. Extension was transferred to the dextral shears, and associated 030° pinnate veins, in a later transtensional stage which promoted connected vein systems and localized fluid-flow. This gave rise to the alteration patterns of the deposit and ore deposition in an area previously affected by the 030° trending Mondoñedo thrust system.

Scaling properties and the geometrical self-affine fractal organization of the shear zones support this interpretation. Vein thickness distributions are generally power-law, and the

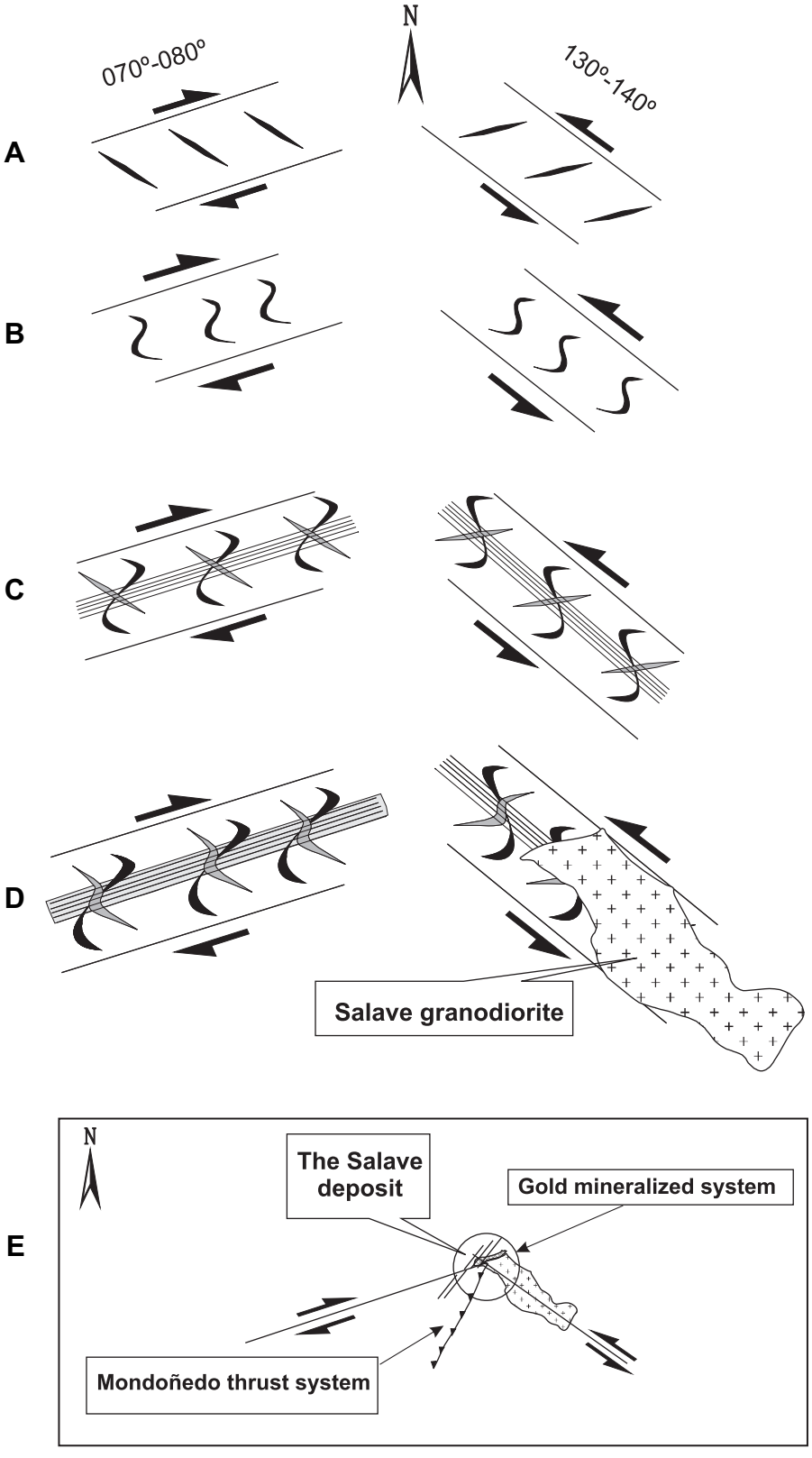

Fig. 7. Idealized model to explain the kinematics evolution of the Punta del Pedrón shear zone related to the Salave deposit (not on scale. For explanation see text).

calculated D_t values ($D_t = 0.81$) from sigmoidal tension gash arrays support that to the east, near the Salave deposit, there are well connected vein systems. Spacing of the sigmoidal tension gashes suggests moderate amounts of clustering, and the calculated D_s values ($D_s = 0.78$) are lower in those systems where extensional components of the shear zones are predominant, promoting the development of connected vein systems, than in those systems where contraction is dominant.

Finally, a geometrical study of semi-brittle to ductile sigmoidal en-échelon tension gash arrays in shear zones utilizing the McCoss (1986) method, with the corresponding assumptions, and the analysis of the scaling properties of vein sets in traverses (lines transecting normal to average vein orientation), both can be utilized in the field to aid in mineral exploration.

Acknowledgements

We are grateful to the Educational and Science Ministry of Spain (MEC) for its financial support through CICYT project numbers HB1997-0034, BTE2003-00290 and MCT-07-BTE62298, and to Jeff Smith for his constructive comments. We also are grateful to John Smith, Thomas Blenkinsop's editorial advise and one anonymous reviewer for many valuable suggestions that notably improved the manuscript.

References

Cepedal, A., Martín-Izard, A., Reguilon, R., Rodrıguez-Pevida, L., Spiering, E., González-Nistal, S., 2000. Origin and evolution of the calcic and magnesian skarns hosting the El Valle-Boinás copper-gold deposit, Asturias (Spain). Journal of Geochemical Exploration 71, 119–151.

Clark, M.B., Brantley, S.L., Fisher, D.M., 1995. Power-law vein thickness distributions and positive feedback in vein growth. Geology 23, 975–978.

Corretgé, G., Suárez, O., 1990. Igneous rocks. In: Dallmeyer, R.D., Martınez-Gracía, E. (Eds.), Pre-Mesozoic Geology of Iberia. Springer-Verlag, Berlin, pp. 72–80.

Fernández-Catuxo, J., 1998. The Salave Gold Prospect revisited: New ideas for an old deposit. In: Arias, D., Martin-Izard, A., Paniagua, A. (Eds.), Gold Exploration and Mining in NW Spain. Facultad de Geologia, Universidad de Oviedo, Oviedo, pp. 82–85.

Fernández-Suárez, J., 1998. Granitoid magmatism in the autochthonous of the NW Iberian Variscan Belt: an overview. In: Arias, D., Martin-Izard, A., Paniagua, A. (Eds.), Gold Exploration and Mining in NW Spain. Facultad de Geologia, Universidad de Oviedo, Oviedo, pp. 12–18.

Fuertes-Fuente, M,, Martın-Izard, A., García-Nieto, J., Maldonado, C., Varela, A., 2000. Preliminary mineralogical and petrological study of the Ortosa Au-Bi-Te ore deposit: a reduced gold skarn in the northern part of the Rıo Narcea Gold Belt, Asturias, Spain. Journal of Geochemical Exploration 71, 177–190.

Gillespie, P.A., Johnston, J.D., Loriga, M.A., McCaffrey, K.J.W., Walsh, J.J., Watterson, J., 1999. Influence of layering on vein systematics in line samples. In: McCaffrey, K.J.W., Lonergan, L., Wilkinson, J.J. (Eds.), Fractures, Fluid Flow and Mineralization. Geological Society, London, Special Publication, 155, pp. 35–56.

Gumiel, P., Campos, R., Sanderson, D.J., Roberts, S., 1995. Geometría y fractalidad de los sistemas filonianos de la mina de La Parrilla (Cáceres): Conectividad y Percolación. Boletín Geológico y Minero 106 (4), 16–37.

Harris, M., 1979. Mineralization at the Salave gold prospect, Asturias, Spain. Ph. D. Thesis, University of London.

Harris, M., 1980a. Gold mineralization at the Salave gold prospect, northwest Spain. Transactions of the Institution of Mining and Metallurgy B 89, 1–4.

Harris, M., 1980b. Hydrothermal alteration at the Salave gold prospect, northwest Spain. Transactions of the Institution of Mining and Metallurgy B 89. 51-15.

Julivert, M., Fontboté, J.M., Ribeiro, A., Nabais Conde, L.E., 1972. Mapa Tectónico de la Península Ibérica y Baleares. Scale. 1:1,000,00. IGME.

Johnston, J.D., McCaffrey, K.J.W., 1996. Fractal properties of vein systems and the variation of scaling relationships with mechanism. Journal of Structural Geology 18, 349–358.

Lang, J.R., Baker, T., 2001. Intrusion-related gold systems: the present level of understanding. Mineralium Deposita 36, 477–489.

Martın-Izard, A., Fuertes-Fuente, M., Cepedal, A., Moreiras, D., García-Nieto, J., Maldonado, C., Pevida, L.R., 2000a. The Río Narcea Gold Belt intrusions: geology, petrology, geochemistry and timing. Journal of Geochemical Exploration 71, 103–117.

Martın-Izard, A., Paniagua, A., García-Iglesias, J., Fuertes-Fuente, M., Boixet, Ll., Maldonado, C., Varela, A., 2000b. The Carles copper-gold-molybdenum skarn (Asturias, Spain): geometry, mineral associations and metasomatic evolution. Journal of Geochemical Exploration 71, 153–175.

Martínez-Catalán, J.R., Pérez-Estaún, A., Bastida, F., Pulgar, J.A., Marcos, A., 1990. West Asturian-Leonese Zone: structure. In: Dallmeyer, R.D., Martínez-García, E. (Eds.), Pre-Mesozoic Geology of Iberia. Springer, pp. 103–114.

McCaffrey, K.J.W., Johnston, J.D., 1996. Fractal analysis of mineralized vein deposit: Curraghinalt gold deposit, County Tyrone. Mineralium Deposita 31, 52–58.

McCoss, A.M., 1986. Simple construction for deformation in transpression/transtension zones. Journal of Structural Geology 8 (6), 715–718.

Nicholson, R., Pollard, D.D., 1985. Dilation and linkage of echelon cracks. Journal of Structural Geology 7 (5), 583–590.

Peacock, D.C.P., Sanderson, D.J., 1995. Pull-aparts, shear fractures and pressure solution. Tectonophysics 241, 1–13.

Pickering, G., Bull, J.M., Sanderson, D.J., 1996. Scaling of fault displacements and implications for estimation of sub-seismic strain. In: Buchanan, P.G., Nieuwland, D.A. (Eds.), Modern Developments in Structural Interpretation, Validation and Modelling. Geological Society Special Publication, 99, pp. 11–26.

Ramsay, J.G., Huber, M.I., 1983. The Techniques of Modern Structural Geology. I: Strain Analysis. Academic Press, London. 307.

Roberts, S., Sanderson, D.J., Gumiel, P., 1998. Fractal analysis of Sn-W mineralization from Central Iberia: insights into the role of fracture connectivity in the formation of an ore deposit. Economic Geology 93 (3), 360–365.

Roberts, S., Sanderson, D.J., Gumiel, P., 1999. Fractal Analysis and Percolation Properties of Veins. In: McCaffrey, K.J.W., Lonergan, L., Wilkinson, J.J. (Eds.), Fractures, Fluid Flow and Mineralization. Geological Society, London, Special Publication, 155, pp. 7–16.

Rodríguez-Terente, L., Paniagua, A., Moreiras, D., 1998. Ore mineralogy and evolution of the Salave Gold Deposit. In: Arias, D., Martin-Izard, A., Paniagua, A. (Eds.), Gold Exploration and Mining in NW Spain. Facultad de Geologia, Universidad de Oviedo, Oviedo, pp. 165–170.

Sanderson, D.J., Roberts, S., Gumiel, P., 1994. A fractal relationship between vein thickness and gold grade in drill-core from La Codosera, Spain. Economic Geology 89, 68–173.

Spiering, E.D., Pevida, L.R., Maldonado, C., Gonzalez, S., Garcıa, J., Varela, A., Arias, D., Martın-Izard, A., 2000. The gold belts of western Asturias and Galicia (NW Spain). Journal of Geochemical Exploration 71, 89–101.